Systematic Analysis of Reactivities and Fragmentation of Glutathione and Its Isomer GluCysGly

ARTICLE *in* THE JOURNAL OF PHYSICAL CHEMISTRY A · APRIL 2014

Impact Factor: 2.69 · DOI: 10.1021/jp501015k · Source: PubMed

6 AUTHORS, INCLUDING:

Xiaoyan Zheng
The Hong Kong University of Science and Tec…
19 PUBLICATIONS **196** CITATIONS
SEE PROFILE

Dong Wang
Tsinghua University
45 PUBLICATIONS **781** CITATIONS
SEE PROFILE

THE JOURNAL OF PHYSICAL CHEMISTRY A

Article

pubs.acs.org/JPCA

Systematic Analysis of Reactivities and Fragmentation of Glutathione and Its Isomer GluCysGly

Shan Feng,[†,∥] Xiaoyan Zheng,[‡,∥] Dong Wang,[‡] Yiyi Gong,[†] Qingtao Wang,[§] and Haiteng Deng*[,†]

[†]MOE Key Laboratory of Bioinformatics, School of Life Sciences, Tsinghua University, Beijing, China

[‡]MOE Key Laboratory of Organic OptoElectronics and Molecular Engineering, Department of Chemistry, Tsinghua University, Beijing, China

[§]Beijing Chaoyang Hospital Affiliated to Capital Medical University, Beijing, China

ABSTRACT: Glutathione (GSH) is the most abundant tripeptide in human cells and plays an important role in protecting cells' integrity against oxidative stress. GSH has an unusual amide linkage formed between the γ-carboxylic group of the glutamic acid in its side-chain and the amine group of cysteine residue. In the present study, we have compared reactivities of GSH to its isomer GluCysGly (ECG), which has a regular amide bond formed between the α-carboxylic group of glutamic acid and the amine group of cysteine residue. The fragmentation pattern of GSH ions in the gas phase is different from that of ECG ions, showing that the loss of H_2O is the major dissociation pathway in ECG fragmentation. This is consistent with the dissociation pathway predicted by density functional calculation. Formation of GSSG from oxidation of GSH is faster than that of ECG disulfide, and the gas phase fragmentation pattern of GSSG is different from that of ECG disulfide. GSH and ECG display similar rates in nucleophilic aromatic substitution when reacting with 1-chloro-2,4-dinitrobenzene (CDNB). However, in the presence of glutathione S-transferases (GST), substitution of CDNB by GSH is 10 times faster than that by ECG. GSH and ECG also show differences in clustering patterns in the gas phase. Taken together, our results shed light on understanding effects of unique boding structure in GSH on its stability and reactivities.

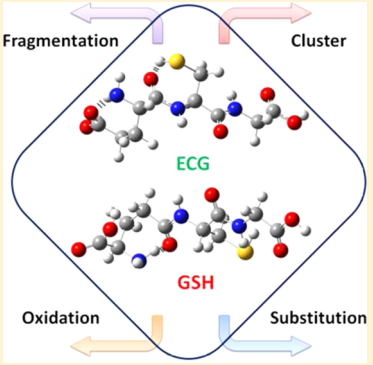

INTRODUCTION

Glutathione (L-γ-glutamyl-L-cysteinylglycine, GSH) is a tripeptide with unique amide bond formed between γ-carboxylic group of the glutamic acid in its side-chain and the amine group of cysteine residue. Synthesis of GSH is a two-step enzymatic process catalyzed by γ-glutamylcysteine synthase and glutathione synthase.[1,2] GSH is the most abundant peptide in mammalian and plant cells and its cellular concentrations reach about 10 mM in cells and about 8 nmol/mg of hemoglobin in blood.[3,4] GSH plays multiple roles in living organisms through the active thiol group in the cysteine residue. Its primary function is to act as an antioxidant against reactive oxygen species (ROS) and endogenous or xenobiotic electrophiles. Glutathione S-transferases (GSTs, EC 2.5.1.18) are the major phase II metabolic enzymes, which can reversibly catalyze the conjugation of the reduced form of glutathione (GSH) to a wide range of xenobiotic substrates and endogenous metabolites.[5,6] The conjugations of xenobiotics with GSH increase their solubility and facilitate their excretion from cells.

Under oxidative stress, GSH can be chemically or enzymatically converted into glutathione disulfide (GSSG). Chemically, direct oxidation of GSH generates a GSH radical and the fusion of GSH radicals forms GSSG.[7,8] Enzymatically, glutathione peroxidases (GPx, EC 1.11.1.9) use GSH as the substrate in reducing hydrogen peroxide or organic peroxides with the production of GSSG, water, or alcohols.[9,10] Peroxiredoxins are a class of enzymes that also use GSH as substrates to reduce hydrogen peroxide.[11,12] GSSG is reduced back to GSH catalyzed by glutathione reductase (GR, EC1.6.4.2) with NADPH as an electron donor. The ratio of GSSG/GSH in combination with other redox-active compounds (e.g., NAD(P)H) defines, regulates, and maintains cellular redox status.[13,14]

Structures, stabilities, and reactivities of GSH have been extensively studied.[15−27] In comparison to other short peptides, GSH is stable in cells due to its unique amide bond formed between γ-carboxyl groups of Glu and amine group of Cys. Intracellular peptidases usually cleave peptide bonds formed by the α-carboxyl groups of amino acids. In the present work, a tripeptide GluCysGly (ECG) with the normal amide bond was synthesized. Using a combination of experimental and theoretical studies, we systematically investigated the differences between stabilities and reactivities of GSH and ECG, and effects of γ-amide bond on reactivities of GSH.

MATERIALS AND METHODS

Materials. GSH and 1-chloro-2,4-dinitrobenzene (CDNB) were purchased from Sigma-Aldrich (St Louis, MO). ECG was

Special Issue: A. W. Castleman, Jr. Festschrift

Received: January 28, 2014
Revised: April 14, 2014

   dx.doi.org/10.1021/jp501015k | J. Phys. Chem. A XXXX, XXX, XXX−XXX

synthesized at WuXi PharmaTech Company (Shanghai, China), and the purity was estimated over 98% by HPLC.

MS/MS Analysis. For MS/MS analysis, GSH and ECG were dissolved in pure water, pH 7.0, and directly sprayed into the Thermo Q Exactive mass spectrometer (Thermo Scientific). Briefly, glass tips (New Objective, MA) with a 2 μm tip diameter were used for nanospray. About 5 μL of samples was loaded into the tip and directly sprayed into a Q Executive mass spectrometer. The temperature of the ion transfer capillary was set at 150 °C and the voltage on S lense was set at 60 V. The electrospray voltage was set up at 1000 V; nitrogen gas was used as the collision gas. MS and MS/MS spectra were acquired in the positive ion mode. Each mass spectrum was analyzed using the Thermo XcaliburQual Browser Software.

Formation Rates of GSSG and ECG Disulfide. The oxidation reactions of GSH and ECG were carried in the presence of 1% or 3% H_2O_2 in 50 mM phosphate buffer (pH 6.5). Formation of GSSG was monitored by A_{260}, of which the extinction coefficient is 240.8 L/mol·cm.[28,29] Briefly, 20 mM GSH or ECG was incubated with H_2O_2 for different time intervals, and A_{260} was measured with a UV/visible spectrophotometer Ultrospec2100 (GE Healthcare). The parameters in rate expression were fit to the experimental data to determine the rate constant k_a.

Nucleophilic Substitution of CDNB by GSH and ECG. HPLC was used to monitor the substitution reaction products, calculated by the peak area at A_{254}. Briefly, 1 mM GSH or ECG was incubated with 1 mM CDNB in 50 mM phosphate buffer (pH 6.5); and the products were analyzed by a 30 min HPLC assay at a flow rate 1 mL/min monitored at 254 nm with a Dionex UltiMate 3000 system (Thermo Scientific). The column was a Vydac 218TP C18 (300 A, 4.6 mm ID, 250 mm length) column. The mobile phase A consisted of methanol with 0.1% trichloroacetic acid, and the mobile phase B consisted of 0.1% trichloroacetic acid in water. The mobile phase was set at 30% of A during HPLC runs. The elution times of CDNB and CDNB−GSH (or CDNB−ECG) were around 15.5 and 6.4 min, respectively. For GST catalyzed nucleophilic substitution, the enzymatic reaction buffer contains 1 mM GSH or ECG and 1 mM CDNB in 50 mM PBS (pH 6.5). The final concentration of enzymes was adjusted to 2 μM. After incubation for 10 min at 37 °C, trichloroacetic acid was added at the final concentration of 0.5% to terminate the catalytic reaction. The enzymatic assays were repeated for three times.

Calculation Methods. The electronic−structure calculations in this work were mainly carried out by the Gaussian 09 package.[30] The recently developed m062x functional with long-range correlation was used in conjunction with the 6-311G** basis set for full geometry optimizations without any symmetry constraint.[31] Normal mode analyses were performed at the same level of theory to ensure that the optimized structures correspond to a true minimum. The bond enthalpies in solution were calculated by using the polarizable continuum model (PCM) in water, with the dielectric constant 78.36.[32]

RESULTS AND DISCUSSION

Structure and Stability of Gas Phase GSH and ECG. Structures of GSH and ECG are displayed in Figure 1. The major difference between these two structures is the distance between the reactive thiol group and the carboxyl or amine group at the peptide N-terminus. The electronic structure

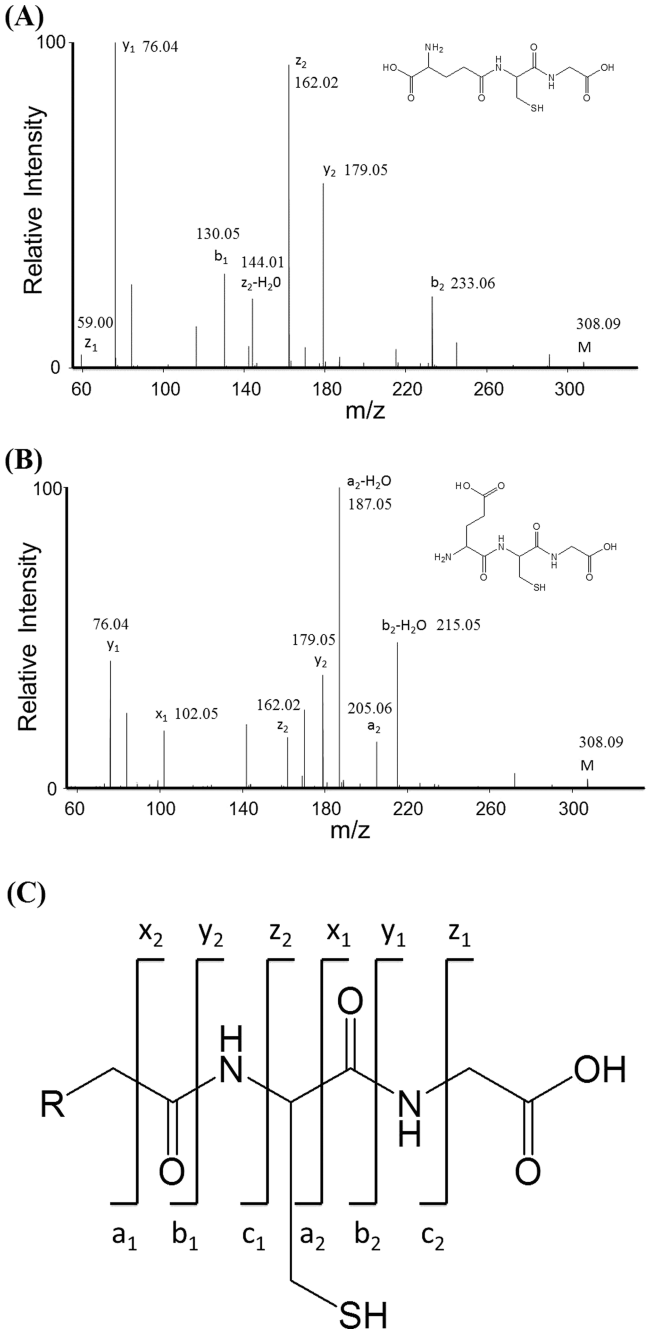

Figure 1. MS/MS spectra of GSH (A) and ECG (B) by collision induced dissociation; and (C) fragmentation pathways of GSH or ECG. R represents the Glu residue.

Table 1. Enthalpy Difference (ΔH) between GSH and ECG, Calculated Following the Formula $\Delta H = H_{GSH} - H_{ECG}$ (kJ/mol)

unit	GSH	ECG	ΔH
Hartree	−1404.7306	−1404.7245	−0.005 689
(kJ/mol)	−3688178.791	−3688163.855	−14.936 469

calculations were carried out by the Gaussian 09 package.[30] The recently developed m062x functional with long-range correlation was used in conjunction with the 6-311G** basis set for full geometry optimizations.[31] On the basis of the known crystal structure of GSH, the enthalpies of GSH and ECG were

dx.doi.org/10.1021/jp501015k | J. Phys. Chem. A XXXX, XXX, XXX−XXX

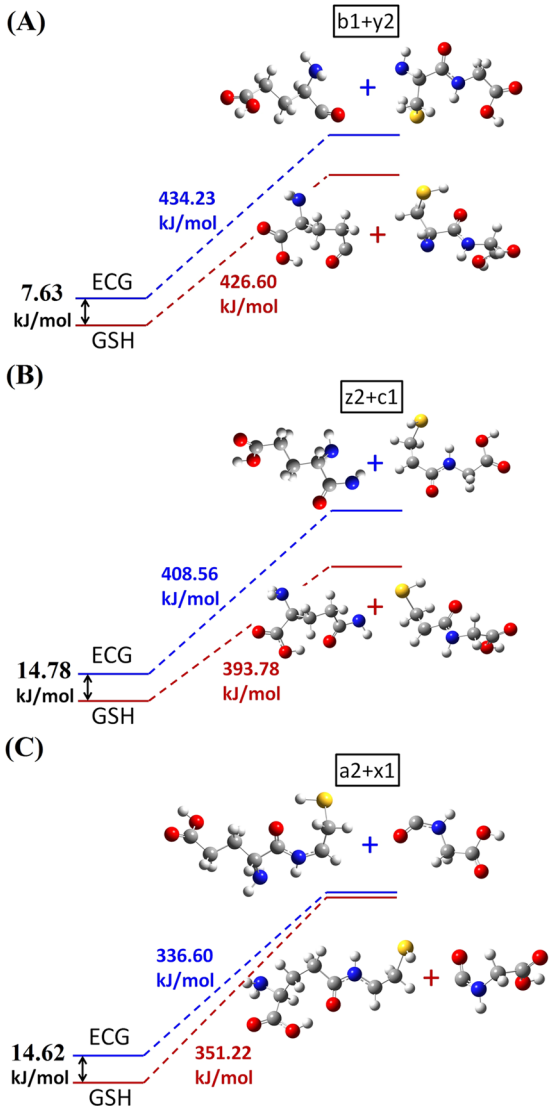

Figure 2. Calculated bond enthalpies in GSH and ECG: (A) b_1 and y_2 fragmentation; (B) c_1 and z_2 fragmentation, and (C) a_2 and x_1 fragmentation.

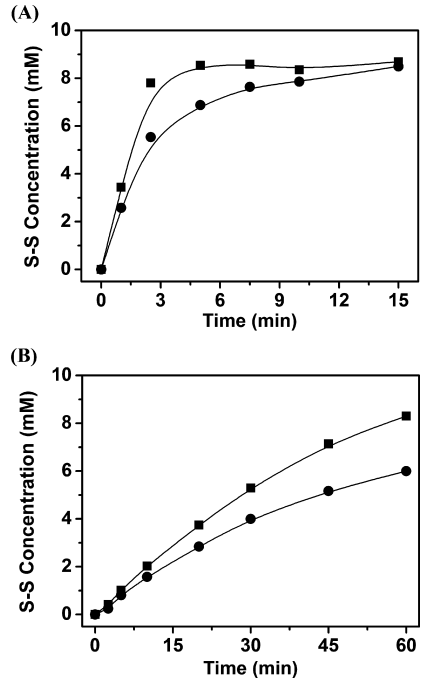

Figure 4. Rates of GSSG and ECG disulfide formation: GSH (square) and ECG (cycle) when oxidized in the presence of 3% H_2O_2 (A) and 1% H_2O_2 (B). The final concentrations of GSH and ECG were 20 mM, and the reactions were carried at 37 °C for 15 and 60 min in the presence of 3% H_2O_2 (A) and 1% H_2O_2 (B), respectively.

calculated (Table 1). The enthalpy of GSH was estimated to be about 15 kJ/mol lower than that of ECG, indicating that GSH is more stable than ECG.

By electrospray mass spectrometry, GSH or ECG ions were detected at 308.091 Da. Under the identical high energy collision dissociation (HCD) conditions, about 95% of precursor ions were fragmented, indicating that both ions had similar stability in the gas phase. However, fragmentation patterns of GSH and ECG are strikingly different (Figure 1). Major fragments of GSH are observed at m/z 179.05 and 162.02, corresponding to y_2 and z_2 ions, while those of ECG are observed at m/z 215.05 and 187.05, corresponding to b_2-18 and a_2-18 ions. We also calculated the bond enthalpies (ΔH) of three different bonds in GSH and ECG peptides, respectively,

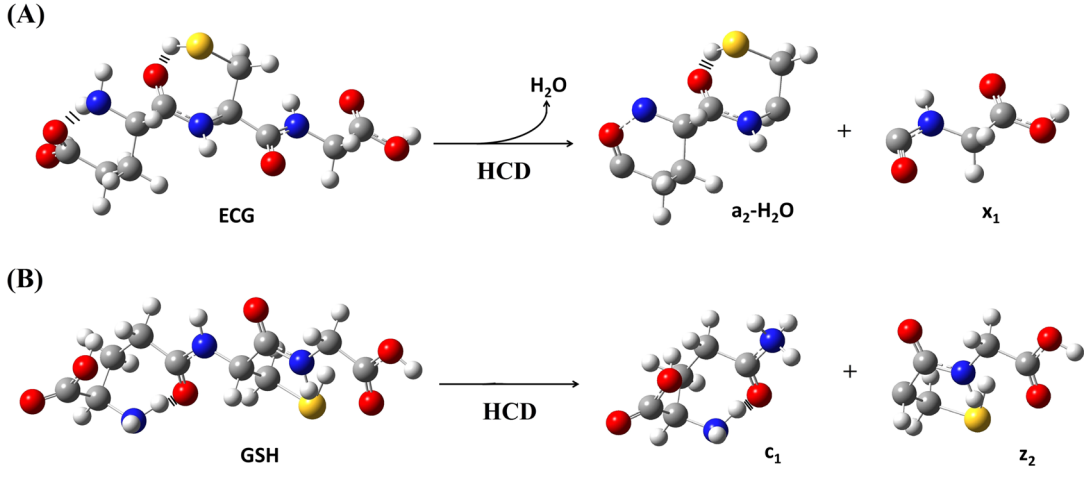

Figure 3. Dissociation intermediates of ECG (A), leading to fragment ions a_2-H_2O and x_1; and GSH (B), leading to fragment ions c_1 and z_2.

dx.doi.org/10.1021/jp501015k | J. Phys. Chem. A XXXX, XXX, XXX−XXX

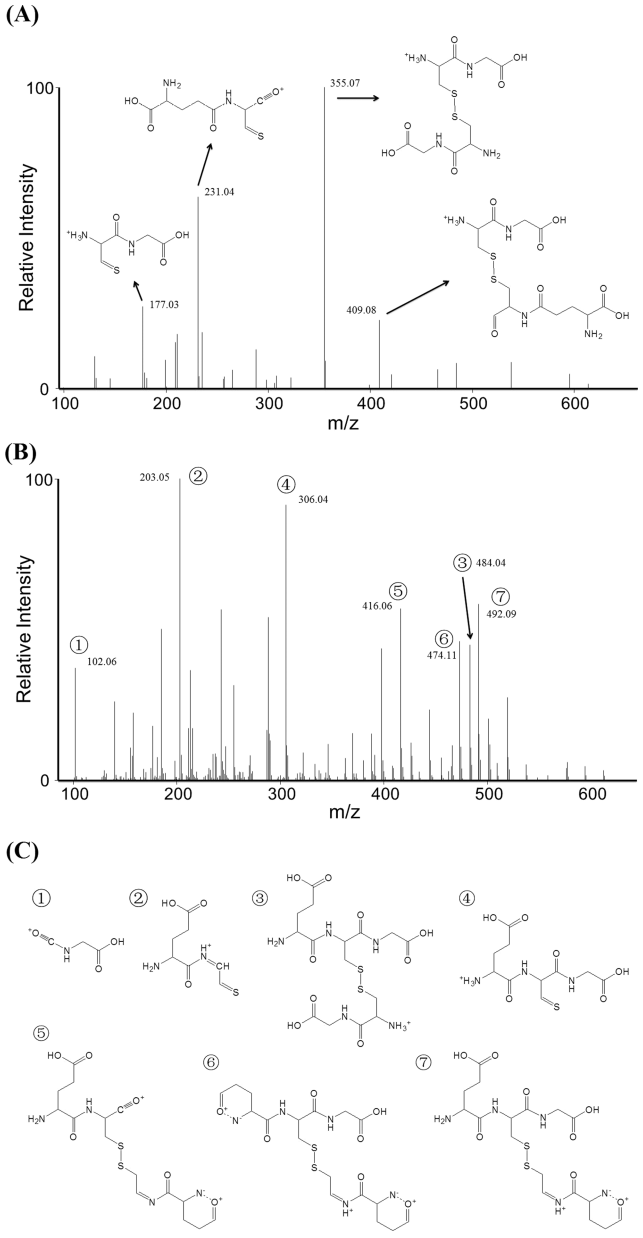

Figure 5. MS/MS spectra of GSSG (A) and ECG disulfide (B) by HCD; (C) structures of fragment ions of ECG disulfide.

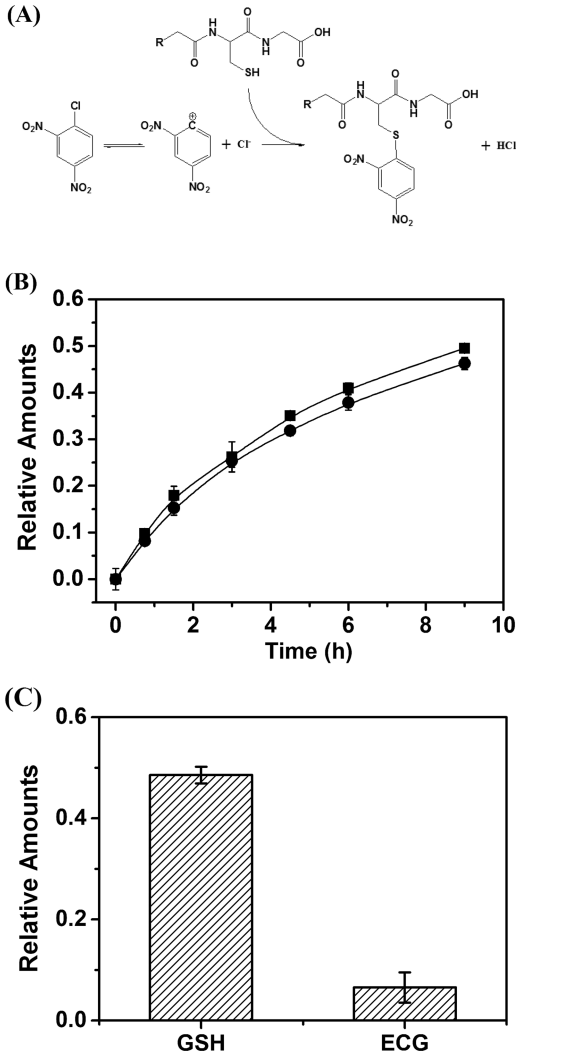

Figure 6. Rates of nucleophilic substitution of GSH and ECG with CDNB. (A) The proposed reaction process of substitution reaction without GST; (B) 1 mM GSH (square) and ECG (cycle) reacting with CDNB at 37 °C for 10 h, the *Y*-axis represents the relative amounts of products measured by HPLC. (B) The relative amounts of the reaction products formed in the presence of 0.2 μM GST for 10 min. The enzymatic assays were repeated for three times.

which lead to three different dissociation pathways (Figure 2). We found that the bond between z_2 and c_1 ions in GSH is weaker than that of ECG, while the bond between a_2 and x_1 fragment ions in ECG has a smaller dissociation energy than that of GSH. The bond enthalpies from theoretical calculations are consistent with our experimental observations. From the fragmentation patterns, structures of the reaction intermediates were proposed (Figure 3). Formation of a hydrogen bond between the α-amine group and the α-carboxyl groups of Glu residue in ECG stabilizes the fragmentation intermediate, leading to the loss of one H_2O molecule and generating the stable a_2-H_2O and x_1 fragments ions. In GSH, the α-amine group and the γ-carbonyl group of Glu form a hydrogen bond leading to stable fragment ions z_2 and c_1.

Formation of GSSG and ECG Disulfide. The major function of GSH is to eliminate ROS. Under oxidative stress, GSH is oxidized to GS radicals that recombine to form GSSG. Under two different concentrations of hydrogen peroxide, we measured the formation rate of GSSG and ECG disulfide. The time-dependent formation of disulfides of GSH and ECG were quantification via A_{260} absorption measurement (Figure 4). GSH has a higher reaction rate to form GSSG as compared to ECG. The second order reaction rates of GSH and ECG were estimated to be 23.29 $L^2/mol^2 \cdot min$ and 11.24 $L^2/mol^2 \cdot min$, respectively, in the presence of 3% of hydrogen peroxide. Since formation of GS radical is the rate-limiting step, the present result suggests that the radical intermediate of GSH is more stable than that of ECG.

A recent theoretical study identified that the O−H bond was the weakest in GSH in the gas phase, while the N−H bond in the ammonium group had the smallest bond dissociation energy (BDE) value in aqueous phase.[18] Furthermore, the cleavage of the O−H or N−H bond was followed by decarboxylation, which made these two processes more energetically favorable over the S−H dissociation. In our experiments, only GSSG or ECG disulfide ions are observed in

dx.doi.org/10.1021/jp501015k | J. Phys. Chem. A XXXX, XXX, XXX−XXX

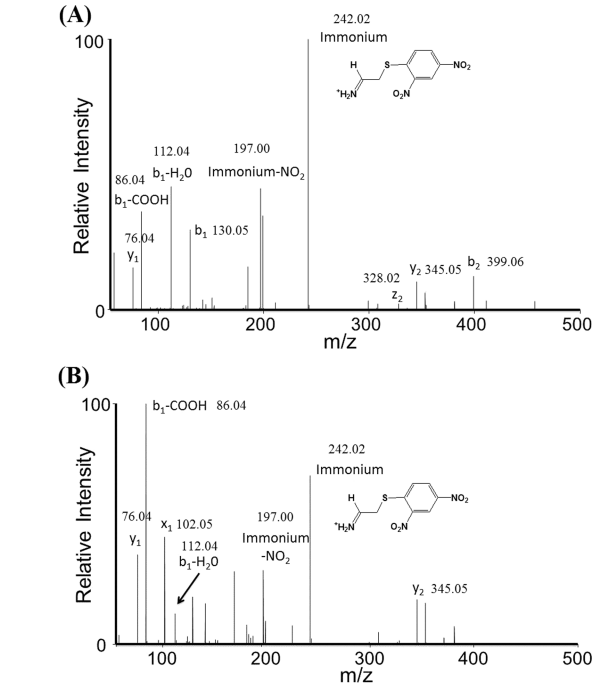

Figure 7. MS/MS spectra of the GSH (A) and ECG (B) substituted CDNB fragmented by HCD.

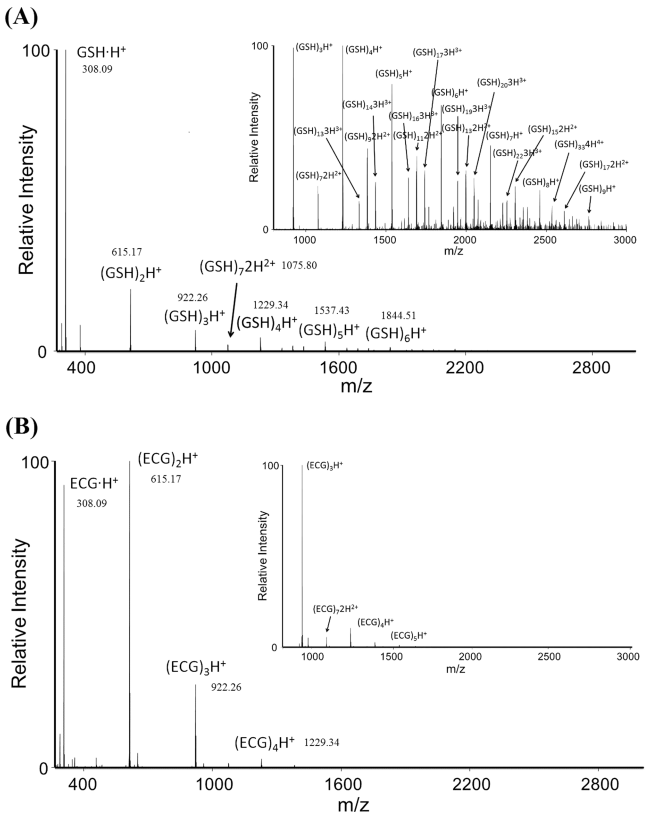

Figure 8. Electrospray mass spectra of clusters of GSH (A) and ECG (B) formed in the gas phase.

mass spectrometry, indicating that the cleavage of S−H bond is the dominant process in oxidation of GSH. However, GSSG and ECG disulfides display different fragmentation patterns under the identical dissociation conditions (Figure 5). The major fragment of GSSG is observed at m/z 355.07 corresponding to the disulfide linked y_2 ions, indicating that the dissociation energy of the disulfide bond is stronger than that of the neighboring amide bond. ECG disulfide displays a complex fragmentation pattern, in which peak 2 and 4 are the most dominant ones by breakage of the disulfide bond (Figure 5B,C). Besides, losses of two H_2O molecules are observed in many fragments. This is consistent with fragmentation of ECG (Figure 1), in which a loss of H_2O is a dominant dissociation pathway.

Nucleophilic Addition of GSH and ECG. Conjugation of GSH with various endogenous or xenobiotic electrophilic compounds is the other function of GSH to protect cells against oxidative stress. One of the reactions is the nucleophilic aromatic substitutions by GSH, in which GSH adducts are formed via displacement of halogen atom with GSH (Figure 6A). Electrospray mass spectrometry confirmed the formation of 1-glutathionyl-2,4-dinitrobenezene resulting from the displacement of the chlorine atom by GSH. We measured the reaction rates of GSH and ECG with 1-chloro-2,4-dinitrobenzene (CDNB), respectively. Without GST catalysis, rates of adduct formation are similar for GSH and ECG (Figure 6B). This suggests that the formation of the radical cation is the rate-limiting step followed by formation of GSH adduct. The reaction process was proposed as illustrated in Figure 6A. In the presence of GST, the formation rate of GSH adduct is 10 times faster than that of ECG adduct (Figure 6C). An earlier study indicated that the formation of the transition state is rate-limiting in the GST-catalyzed nucleophilic aromatic substitution reactions.[33] The slow reaction rate of GST-catalyzed ECG substitution indicates that the GSH-binding packet in GST may have steric hindrance for binding ECG.

Tandem mass spectrometry was carried out to dissociate GSH− or ECG−dinitrobenzene (Figure 7). Both ions show a similar fragmentation pattern, in which the major fragment was observed at m/z 242.02 corresponding to the dinitrobenzene modified Cys immonium ion. The structure of this fragment is displayed in Figure 7, which further loses a NO_2 molecule to generate an additional fragment at m/z 197.00. Cleavage of the C−S bond between dinitrobenzene and the thiol group is not observed; consistent with the earlier study that examined fragmentation of 19 aromatic GSH conjugates.[25] Our results provide new information for understanding interactions of amino acid residues in the catalytic center of GST and GSH.

Formation of Noncovalent Oligomers of GSH and ECG in the Gas Phase. Using electrospray mass spectrometry, we analyzed proton-binded oligomers of GSH and ECG in the gas phase. Different clustering patterns were observed for GSH and ECG (Figure 8). GSH tends to form the large clusters. The clusters with up to 33 GSH subunits were observed in mass spectrometry. However, the clusters of ECG only have a few ECG subunits. The intensity ratio of $(GSH)_2H^+$ to $GSH{\cdot}H^+$ is about 0.2; however, it is about 1 for ECG, indicating that noncovalent dimer of ECG is more stable. An earlier study reported that glutathione interacted with Met, Phe, Tyr, Ser, or Ile to form noncovalent complexes with different affinity.[34] Our experiments showed that both GSH and ECG formed noncovalent oligomers. On the basis of the enthalpy difference, GSH is more stable than ECG, while ECG is facile to form a dimer as observed in mass spectra in Figure 8.

Tandem mass spectrometry was employed to investigate the dissociation of $(GSH)_4H^+$ in the gas phase. MS/MS spectra of $(GSH)_4H^+$ and $(ECG)_4H^+$ are displayed in Figure 9. Under the identical experimental conditions with the lower collision

dx.doi.org/10.1021/jp501015k | J. Phys. Chem. A XXXX, XXX, XXX−XXX

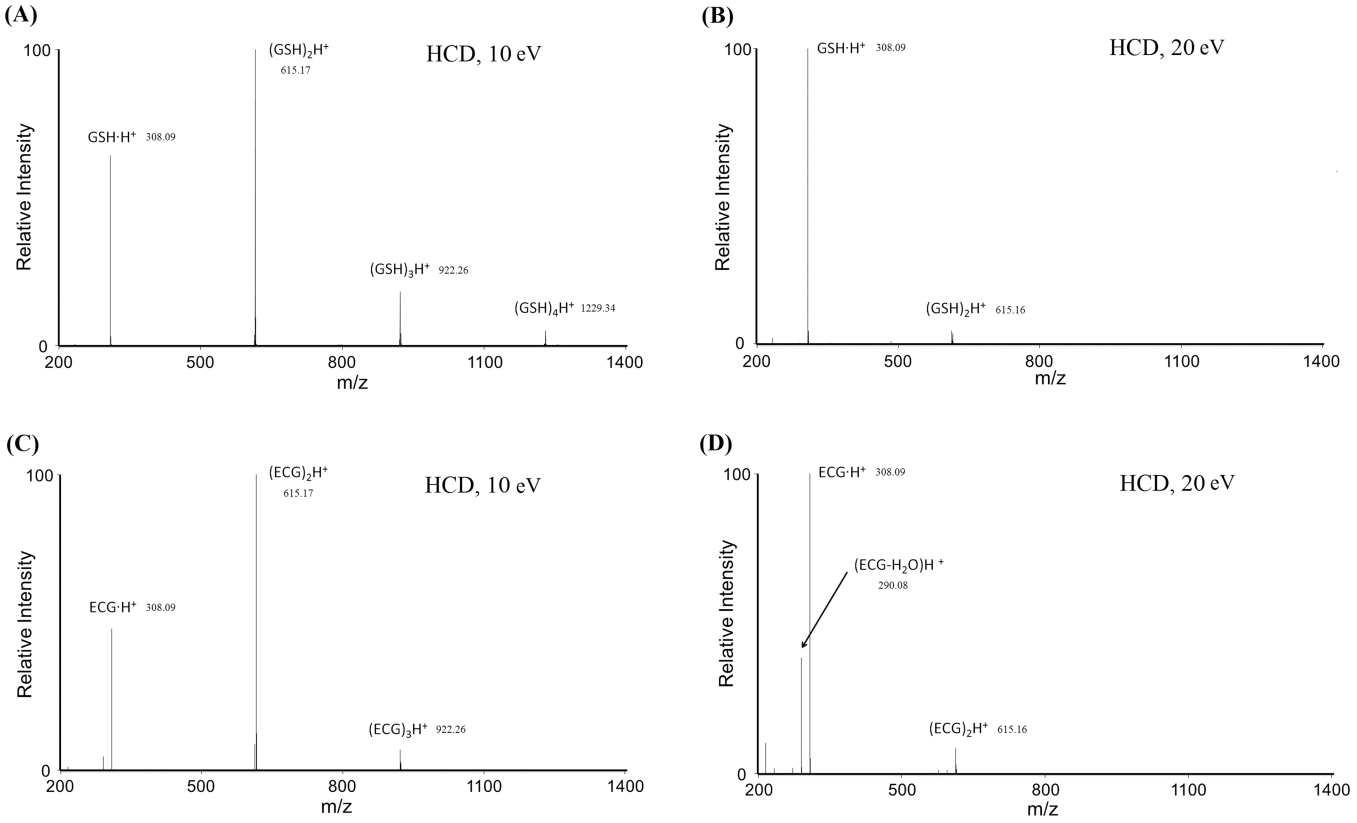

Figure 9. MS/MS spectra of $(GSH)_4H^+$ and $(ECG)_4H^+$ fragmentation at different collision energies. (A) GSH, 10 eV; (B) GSH, 20 eV; (C) ECG, 10 eV; (D) ECG, 20 eV.

energy (10 eV), both clusters show similar fragmentation patterns. However, at the collision energy 20 eV, a fragment at m/z 290.08 is only observed in ECG fragmentation, which corresponds to a loss of water molecule from ECG, consistent with the calculation results showing that GSH is more stable than ECG.

CONCLUSIONS

Taken together, systematic analysis of dissociation and reactivities of GSH and its isomer ECG showed that fragmentation of ECG favors a loss of H_2O molecule and that GSH has a higher reactivity to form disulfide. In GST-catalyzed nucleophilic substitution, the reaction rate of GSH is 10 times higher than that of ECG, suggesting the steric hindrance in ECG−GST binding. Our results demonstrate that the unique amide bond between glutamic acid and cysteine in GSH affects its stability, structure, and reactivities and further influence the antioxidant functions of GSH.

AUTHOR INFORMATION

Corresponding Author

*(H.D.) E-mail: dht@mail.tsinghua.edu.cn. Tel: 8610-62790498.

Author Contributions

‖These authors (S.F. and X.Z.) contributed equally to this work.

Notes

The authors declare no competing financial interest.

ACKNOWLEDGMENTS

We thank the Protein Chemistry Facility at the Center for Biomedical Analysis of Tsinghua University for sample analysis and the Tsinghua Supercomputing Center for computational resources. This work was supported in part by NSFC 31270871 (to H.D.), 21273124 (to D.W.), and MOEC 2012Z02A549 (to H.D).

REFERENCES

(1) Lushchak, V. I. Glutathione Homeostasis and Functions: Potential Targets for Medical Interventions. *J. Amino Acids* **2012**, *2012*, 736837.

(2) Dickinson, D. A.; Forman, H. J. Cellular Glutathione and Thiols Metabolism. *Biochem. Pharmacol.* **2002**, *64*, 1019−1026.

(3) Schafer, F. Q.; Buettner, G. R. Redox Environment of the Cell as Viewed through the Redox State of the Glutathione Disulfide/Glutathione Couple. *Free Radic. Biol. Med.* **2001**, *30*, 1191−1212.

(4) Pastore, A.; Piemonte, F.; Locatelli, M.; Russo, A. L.; Gaeta, L. M.; Tozzi, G.; Federici, G. Determination of Blood Total, Reduced, and Oxidized Glutathione in Pediatric Subjects. *Clin. Chem.* **2001**, *47*, 1467−1469.

(5) Brunton, L. L.; Lazo, J. S.; Parker, K. L. *The Pharmacological Basis of Therapeutics*, 12th ed.; McGraw-Hill: New York, 2005; p 73.

(6) Jakoby, W.; Ziegler, D. The Enzymes of Detoxication. *J. Biol. Chem.* **1990**, *265*, 20715−20718.

(7) Winterbourn, C. C. Superoxide as an Intracellular Radical Sink. *Free Radic. Biol. Med.* **1993**, *14*, 85−90.

(8) Jones, C.; Lawrence, A.; Wardman, P.; Burkitt, M. Kinetics of Superoxide Scavenging by Glutathione: An Evaluation of Its Role in the Removal of Mitochondrial Superoxide. *Biochem. Soc. Trans.* **2003**, *31*, 1337−1340.

(9) Cohen, G.; Hochstein, P. Glutathione Peroxidase: The Primary Agent for the Elimination of Hydrogen Peroxide in Erythrocytes. *Biochemistry* **1963**, *2*, 1420−1428.
(10) Brigelius-Flohé, R. Tissue-Specific Functions of Individual Glutathione Peroxidases. *Free Radic. Biol. Med.* **1999**, *27*, 951−965.
(11) Rhee, S. G.; Chae, H. Z.; Kim, K. Peroxiredoxins: A Historical Overview and Speculative Preview of Novel Mechanisms and Emerging Concepts in Cell Signaling. *Free Radic. Biol. Med.* **2005**, *38*, 1543−1552.
(12) Egler, R. A.; Fernandes, E.; Rothermund, K.; Sereika, S.; de Souza-Pinto, N.; Jaruga, P.; Dizdaroglu, M.; Prochownik, E. V. Regulation of Reactive Oxygen Species, DNA Damage, and C-Myc Function by Peroxiredoxin 1. *Oncogene* **2005**, *24*, 8038−8050.
(13) Janssen-Heininger, Y. M.; Mossman, B. T.; Heintz, N. H.; Forman, H. J.; Kalyanaraman, B.; Finkel, T.; Stamler, J. S.; Rhee, S. G.; van der Vliet, A. Redox-Based Regulation of Signal Transduction: Principles, Pitfalls, and Promises. *Free Radic. Biol. Med.* **2008**, *45*, 1−17.
(14) Bánhegyi, G.; Margittai, É.; Szarka, A.; Mandl, J.; Csala, M. Crosstalk and Barriers between the Electron Carriers of the Endoplasmic Reticulum. *Antioxid. Redox Signaling* **2012**, *16*, 772−780.
(15) Cubas, M. L.; Ventura, O. N. A Conformational Study of the Hemimercaptal of Methylglyoxal and Glutathione Including the Study of Solvent Effects. *J. Braz. Chem. Soc.* **1991**, *2*, 111−117.
(16) Wolfe, S.; Weaver, D. F.; Yang, K. Mmpep: Development and Evaluation of Peptide Parameters for Allinger's Mmp2 (85) Programme, Including Calculations on Crambin and Insulin. *Can. J. Chem.* **1988**, *66*, 2687−2702.
(17) Ko, Y. J.; Wang, H.; Li, X.; Bowen, K.; Lecomte, F.; Desfrançois, C.; Poully, J. C.; Grégoire, G.; Schermann, J. P. Intrinsic Neutral and Anionic Structures of Glutathione. *ChemPhysChem* **2009**, *10*, 3097−3100.
(18) Fiser, B. L.; Szőri, M. N.; Jójárt, B. Z.; Izsák, R. B.; Csizmadia, I. G.; Viskolcz, B. L. Antioxidant Potential of Glutathione: A Theoretical Study. *J. Phys. Chem. B* **2011**, *115*, 11269−11277.
(19) Fiser, B.; Jójárt, B.; Csizmadia, I. G.; Viskolcz, B. Glutathione−Hydroxyl Radical Interaction: A Theoretical Study on Radical Recognition Process. *PloS One* **2013**, *8*, e73652.
(20) Tan, L.; Xia, Y. Gas-Phase Reactivity of Peptide Thiyl ($Rs^{\bullet}$), Perthiyl ($Rss^{\bullet}$), and Sulfinyl ($Rso^{\bullet}$) Radical Ions Formed from Atmospheric Pressure Ion/Radical Reactions. *J. Am. Soc. Mass Spectrom.* **2013**, *24*, 534−542.
(21) Zhao, J.; Siu, K. M.; Hopkinson, A. C. Glutathione Radical Cation in the Gas Phase; Generation, Structure and Fragmentation. *Org. Biomol. Chem.* **2011**, *9*, 7384−7392.
(22) Thakur, S. S.; Balaram, P. Fragmentation of Peptide Disulfides under Conditions of Negative Ion Mass Spectrometry: Studies of Oxidized Glutathione and Contryphan. *J. Am. Soc. Mass Spectrom.* **2008**, *19*, 358−366.
(23) Osburn, S.; Berden, G.; Oomens, J.; Gulyuz, K.; Polfer, N. C.; O'Hair, R. A.; Ryzhov, V. Structure and Reactivity of the Glutathione Radical Cation: Radical Rearrangement from the Cysteine Sulfur to the Glutamic Acid A-Carbon Atom. *ChemPlusChem* **2013**, *78*, 970−978.
(24) Murphy, C. M.; Fenselau, C.; Gutierrez, P. L. Fragmentation Characteristic of Glutathione Conjugates Activated by High-Energy Collisions. *J. Am. Soc. Mass Spectrom.* **1992**, *3*, 815−822.
(25) Xie, C.; Zhong, D.; Chen, X. A Fragmentation-Based Method for the Differentiation of Glutathione Conjugates by High-Resolution Mass Spectrometry with Electrospray Ionization. *Anal. Chim. Acta* **2013**, *788*, 89−98.
(26) Schwöbel, J.; Madden, J.; Cronin, M. Examination of Michael Addition Reactivity Towards Glutathione by Transition-State Calculations. *SAR QSAR Environ. Res.* **2010**, *21*, 693−710.
(27) Singh, B. K. Complexation Behavior of Glutathione with Metal Ions. *Asian J. Chem.* **2005**, *17*, 1−32.
(28) Wetlaufer, D. Ultraviolet Spectra of Proteins and Amino Acids. *Adv. Protein Chem.* **1962**, *17*, 303−390.
(29) Bailey, J. UV Absorption Characteristics of *N*-Acetyl Methyl Esters of the Aromatic Amino Acids, Cystine, and *N*-Acetylcysteine. In *Handbook of Biochemistry*; Chemical Rubber Co.: Cleveland, OH, 1968; p B-18.
(30) Frisch, M.; Trucks, G.; Schlegel, H. B.; Scuseria, G.; Robb, M.; Cheeseman, J.; Scalmani, G.; Barone, V.; Mennucci, B.; Petersson, G.; et al. *Gaussian 09*; Gaussian Inc.: Wallingford, CT, 2009.
(31) Zhao, Y.; Truhlar, D. G. The M06 Suite of Density Functionals for Main Group Thermochemistry, Thermochemical Kinetics, Noncovalent Interactions, Excited States, and Transition Elements: Two New Functionals and Systematic Testing of Four M06-Class Functionals and 12 Other Functionals. *Theor. Chem. Acc.* **2008**, *120*, 215−241.
(32) Tomasi, J.; Mennucci, B.; Cammi, R. Quantum Mechanical Continuum Solvation Models. *Chem. Rev.* **2005**, *105*, 2999−3094.
(33) Patskovsky, Y.; Patskovska, L.; Almo, S. C.; Listowsky, I. Transition State Model and Mechanism of Nucleophilic Aromatic Substitution Reactions Catalyzed by Human Glutathione S-Transferase M1a-1a. *Biochemistry* **2006**, *45*, 3852−3862.
(34) Dai, Z. Y.; Chu, Y. Q.; Wu, B.; Wu, L.; Ding, C. F. Investigation of Non-Covalent Complexes of Glutathione with Common Amino Acids by Electrospray Ionization Mass Spectrometry. *Acta Pharmacol. Sin.* **2008**, *29*, 759−711.